

# Probing scalar meson structures in $\chi_{c1}$ decays into pseudoscalar and scalar

Qian Wang<sup>1</sup>, Gang Li<sup>2</sup>, and Qiang Zhao<sup>1,3</sup>

1) *Institute of High Energy Physics, Chinese Academy of Sciences, Beijing 100049, P.R. China*

2) *Department of Physics, Qufu Normal University, Qufu, 273165, P.R. China*

3) *Theoretical Physics Center for Science Facilities, CAS, Beijing 100049, China*

(Dated: March 12, 2018)

We evaluate the decay branching ratios of  $\chi_{c1} \rightarrow PS$ , in a quark model parametrization scheme, where  $P$  and  $S$  stand for pseudoscalar and scalar meson, respectively. An interesting feature of this decay process is that the  $c\bar{c}$  annihilate via the pQCD hair-pin diagram is supposed to be dominant. Hence, this decay process should be sensitive to the quark components of the final-state light mesons, and would provide a great opportunity for testing the mixing relations among the scalar mesons, i.e.  $f_0(1370)$ ,  $f_0(1500)$  and  $f_0(1710)$ , by tagging the final state pseudoscalar mesons.

PACS numbers: 13.25.Gv, 12.39.Mk, 12.39.St

## I. INTRODUCTION

The usefulness of charmonium hadronic decays into light mesons is that this transition occurs via a gluon-rich process. The initial charm and anti-charm quark will annihilate into gluons and light quarks will be produced in the final state through the hadronization of intermediate gluons. For the interest of studying the structure of the final state light mesons, especially in order to search for signals for glueball candidates, the hadronic decays of charmonium system provides an ideal platform on which the production of exotic states can be correlated with a relatively well-understood state. Such a tag sometimes exposes unexpected phenomena for which various possible mechanisms can be examined. Review of heavy quarkonium dynamics can be found in Refs. [1, 2].

In the charmonium sector there are several recent observations pertaining to scalar meson production in charmonium decays which turn out to be unexpected. One is the BES-II results for  $J/\psi \rightarrow \phi f_0^i$  [3] and  $\omega f_0^i$  [4], ( $i = 1, 2, 3$  labels  $f_0(1370)$ ,  $f_0(1500)$  and  $f_0(1710)$ ), which show that the branching ratio of  $J/\psi \rightarrow \phi f_0(1710)$  is smaller than that of  $J/\psi \rightarrow \omega f_0(1710)$ . In contrast, the branching ratio of  $J/\psi \rightarrow \omega f_0(1370)$  is smaller than  $\phi f_0(1370)$ . The paradox arising here is that  $f_0(1710)$  dominantly decays into  $K\bar{K}$ , hence is usually believed to have a large  $s\bar{s}$  component. Therefore, one would naturally expect that the production of  $f_0(1710)$  recoiled by the  $\phi$  meson should be favored than recoiled by the  $\omega$  due to the OZI rule. Similar paradox occurs to the  $f_0(1370)$  which is strongly coupled to  $4\pi$  and believed to be dominated by a non-strange  $q\bar{q}$  component. Efforts have been made in the literature to explore the properties of these scalar mesons and their mixings [5–10].

The other experimental observation comes from CLEO-c [11] and BES-II measurements [12–17] of  $\chi_{c0,2}$  decays into meson pairs. It shows that the decay channels of  $\chi_{c0,2} \rightarrow PP$  and  $VV$  still respect the OZI rule well and the DOZI processes are much suppressed [18, 19]. As a consequence, the leading transition amplitude is given by the singly OZI disconnected (SOZI) transitions, and the decay branching ratios for  $\chi_{c0,2} \rightarrow PP$  and  $VV$  still fit the pattern of SU(3) flavor symmetry. In contrast, in the channel where scalar isoscalar  $f_0$  states are produced, there are obvious deviations from the expectation of the OZI rule. In particular, the BES-II measurement [17] shows that one of the largest branching ratios is from  $\chi_{c0} \rightarrow f_0(1370)f_0(1710)$  for  $\chi_{c0,2} \rightarrow SS$  which greatly violate the OZI rule expectation. As pointed out in Ref. [18], such a deviation could be a strong evidence for the glueball- $q\bar{q}$  mixing in the scalar isoscalar wavefunctions. Nevertheless, the scalar production is correlated with the large OZI-rule breaking in the DOZI processes as a common dynamic feature.

Compared to  $\chi_{c0,2}$  decays into two gluons, the two gluon annihilations of the  $\chi_{c1}$  in perturbative QCD is suppressed by the Landau-Yang theorem [20] in the on-shell limit for those two gluons. As a result, the annihilations would be dominated by the pQCD hair-pin diagram as shown in Fig. 1(a) instead of the connected diagram (Fig. 1(b)). As studied in Ref. [21], due to the Landau-Yang theorem, the total width of  $\chi_{c1}$  is suppressed and nearly saturated by the hair-pin diagram where the two gluons are not necessarily to be on shell simultaneously. The strong suppression on the connected diagram (Figs. 1(b)-(e)) can be understood by the following analyses. As a comparison, let us first take a look at the decays of  $\chi_{c0,2} \rightarrow 2g$ , where Fig. 1(b) generally plays an important role [22]. In a view of quark-hadron duality, this process can be treated as a two-step process, e.g.  $c\bar{c}(0^{++}) \rightarrow 2g \rightarrow q\bar{q}(0^{++})$  and then the creation of the second quark pair to form final-state hadrons. The first step is analogue to a mixing process that the first light quark pair is saturated by all the  $q\bar{q}$  configurations with  $J^{PC} = 0^{++}$ . The second  $q\bar{q}$  pair is

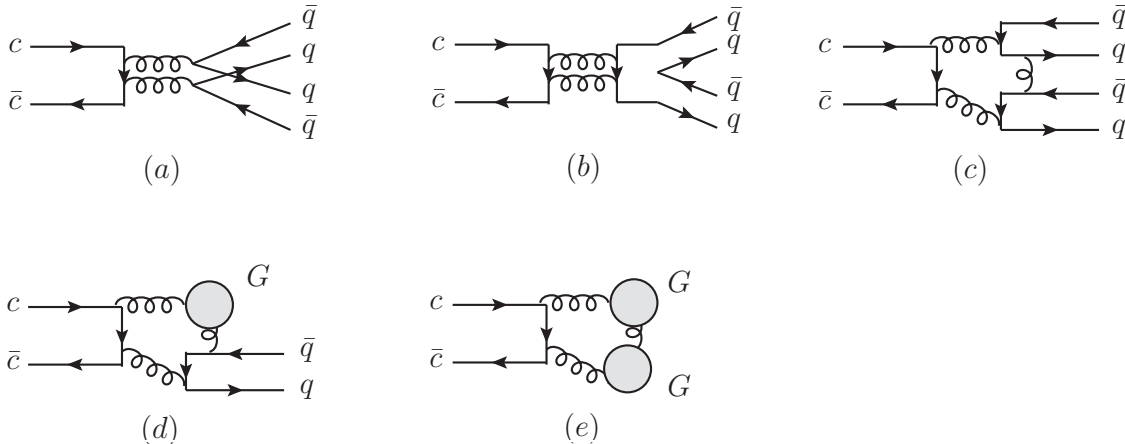


FIG. 1: The schematic Feynman diagrams of  $\chi_{c1} \rightarrow PS$  via two-gluon annihilations.

produced via non-perturbative quark pair creation for which the present calculations are generally in the quark model framework [22]. The dominant contributions from e.g. Fig. 1(b) in  $\chi_{c0,2}$  decays are because of the enhancement of the first step transition, i.e.  $c\bar{c}(0^{++}) \rightarrow 2g \rightarrow q\bar{q}(0^{++})$ , when those two gluons are both on shell. In contrast, the  $\chi_{c1}$  decays via Fig. 1(b) with the on-shell gluons are forbidden by the Landau-Yang theorem. Since the integrands of those gluon connected diagrams drop quickly when the gluon momentum goes off shell, such a critical constraint has strongly suppressed the contributions from those gluon connected processes, i.e. Figs. 1(b)-(e), as a general character for the exclusive decays of  $\chi_{c1}$ . We note that there is a gluon hair-pin diagram in association with Fig. 1(e) where the gluons must be off shell and can be directly connected to the final state glueball components of the pseudoscalar and scalar mesons. However, this process is relative suppressed by the strong  $\alpha_s$  in respect to Fig. 1(e) because of the additional three-gluon vertices. Also, notice that the glueball components inside  $\eta$  and  $\eta'$  are rather small. We regard contributions from such a process as subleading ones. In this work, we only consider  $\eta$  and  $\eta'$  as the flavor singlet and octet mixing states.

The following features can be further recognized: i) Figure 1(c) will suffer from OZI doubly disconnected (DOZI) suppression due to the large recoil momentum carried by the exchanged gluon between the quarks in the final state. ii) Figures 1(d) and (e) may gain an enhancement by the gluon powers considering that the gluon couplings to the glueball generally do not pay a price. However, note that the total width of  $\chi_{c1}$  is nearly saturated by Fig. 1(a), it is confident to conclude that the DOZI and Landau-Yang suppression still play a dominant role here. We caution that the neglect of Figs. 1(b)-(e) is based on qualitative argument and experimental observations. Detailed model studies of those processes are still needed to provide a quantitative prescription.

The three gluon annihilations of  $\chi_{c1}$  into  $PS$  are also highly suppressed. One reason is because of the increase of the gluon powers. The other reason is that at least one of the final state meson will be produced via higher-twist components in the wavefunction as illustrated in Fig. 2. Based on the above considerations, it should be a reasonable approximation to treat the hair-pin diagram as the leading contribution to  $\chi_{c1} \rightarrow PS$ .

In this work, we will show that by tagging the quark components of  $\eta$  and  $\eta'$  in the final state, it is possible to investigate the quark components of the scalar mesons in  $\chi_{c1} \rightarrow PS$ . In particular, this process turns out to be sensitive to the glueball and  $q\bar{q}$  mixing pattern. Therefore, it can be selective for different mixing schemes and serve as an alternative way to study the structure of scalar mesons.

As follows, we first give details of the parametrization scheme in Sec. II. The numerical results are presented in Sec. III, and a brief summary is given in the last section.

## II. PARAMETRIZATION SCHEME

A systematic parametrization scheme has been exploited for various charmonium hadronic decays [18, 19, 23], where the SOZI and DOZI processes can be parameterized out based on gluon counting rules. Those parameters can then be

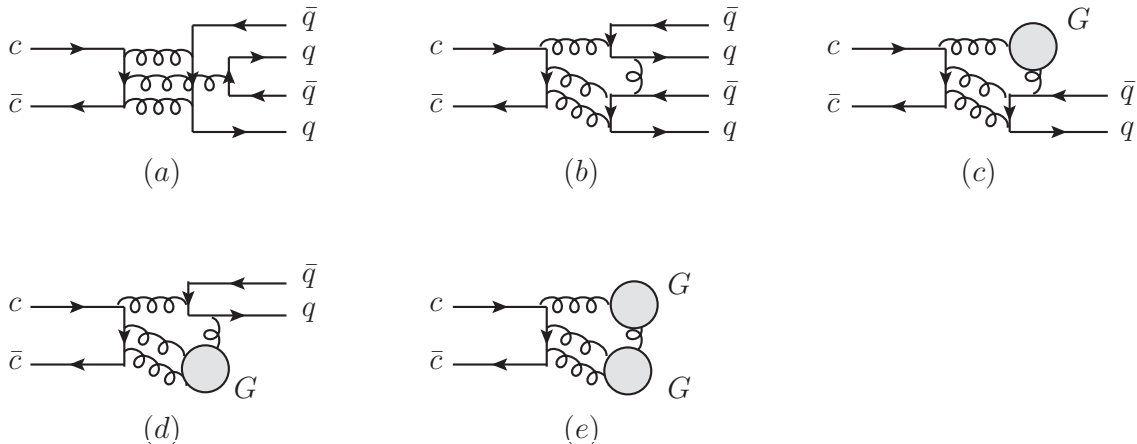


FIG. 2: The schematic Feynman diagrams of  $\chi_{c1} \rightarrow PS$  via three-gluon annihilations.

determined by experimental data from which predictions can be made for unmeasured channels. Early works based on similar parametrization can be found in Refs. [5–8]. In the case of  $\chi_{c1} \rightarrow PS$ , as discussed in the Introduction, the dominant contribution is from Fig. 1(a) while the others are supposed to be strongly suppressed because of the Landau-Yang theorem. It makes the parametrization rather simple as we will detail below.

For the production of isoscalar pseudoscalar mesons, since it has been well established that the glueball components inside  $\eta$  and  $\eta'$  are rather small, it should be a good approximation to neglect their possible internal glueball components, and simply take the quark mixings in the SU(3) flavor basis:

$$\eta = \cos \alpha_P |n\bar{n}\rangle - \sin \alpha_P |s\bar{s}\rangle, \quad (1)$$

$$\eta' = \sin \alpha_P |n\bar{n}\rangle + \cos \alpha_P |s\bar{s}\rangle, \quad (2)$$

where  $\alpha_P = \theta_P + \arctan \sqrt{2}$  and  $\theta_P$  is usually considered to be  $-22^\circ \sim -13^\circ$ . Here we adopt the commonly used value  $\theta_P = -19^\circ$  to evaluate the branching ratios. With this mixing scheme, we eventually use the pseudoscalar mesons  $\eta$  and  $\eta'$  as a flavor tag for the production of the quark components of the scalar mesons via Fig. 1(a), while contributions from other processes can be neglected.

The rich spectrum of scalar mesons in the mass region of 1~2 GeV has initiated a lot of studies of the scalar mesons including the search for the scalar glueball candidate (see Refs. [24, 25] and references therein). A broadly discussed scenario is the glueball- $q\bar{q}$  mixing among those three scalars, i.e.  $f_0(1370)$ ,  $f_0(1500)$  and  $f_0(1710)$ . In the SU(3) flavor basis, these states as the eigenstates of  $n\bar{n}$ ,  $s\bar{s}$  and  $G$  components can be generally expressed as

$$\begin{pmatrix} |f_0(1710)\rangle \\ |f_0(1500)\rangle \\ |f_0(1370)\rangle \end{pmatrix} = \hat{S} \begin{pmatrix} |G\rangle \\ |s\bar{s}\rangle \\ |n\bar{n}\rangle \end{pmatrix} = \begin{pmatrix} x_1 & y_1 & z_1 \\ x_2 & y_2 & z_2 \\ x_3 & y_3 & z_3 \end{pmatrix} \begin{pmatrix} |G\rangle \\ |s\bar{s}\rangle \\ |n\bar{n}\rangle \end{pmatrix}, \quad (3)$$

where  $x_i$ ,  $y_i$  and  $z_i$  are the mixing matrix elements determined by mixing mechanisms. Different models have different solutions for the mixing matrix [5–8, 10, 26]. A critical difference among those mixing schemes focuses on the magnitude of glueball components inside  $f_0(1710)$  and  $f_0(1500)$ , and in contrast, all those mixing schemes seem to agree that the  $f_0(1370)$  is dominated by the  $n\bar{n}$  component. Unfortunately, there still lack unique criteria for identifying the scalar glueball state and distinguish those mixing schemes.

With  $V_a$  standing for the potential of the SOZI process, a basic transition parameter  $g$  can be defined as

$$g \equiv \langle (q\bar{q})_P (q\bar{q})_S | V_a | \chi_{c1} \rangle, \quad (4)$$

where  $q$  ( $\bar{q}$ ) is a non-strange quark (antiquark). Considering the SU(3) flavor symmetry breaking, which distinguishes an  $s$  quark pair production from the  $u/d$  quarks in the hadronizations, we introduce the SU(3) flavor symmetry breaking parameter  $R$ ,

$$R \equiv \frac{\langle (s\bar{q})_P (q\bar{s})_S | V_a | \chi_{c1} \rangle}{\langle (q\bar{q})_P (q\bar{q})_S | V_a | \chi_{c1} \rangle}, \quad (5)$$

where  $R = 1$  is in the SU(3) flavor symmetry limit, while deviations from unity implies the SU(3) flavor symmetry breaking. In general, the value of parameter  $R$  is around  $R \simeq f_\pi/f_K = 0.838$ , which provides a guidance for the SU(3) flavor symmetry breaking effects. For the creation of two pairs of  $s\bar{s}$  via the SOZI process, the recognition of the SU(3) flavor symmetry breaking in the transition is

$$R^2 = \frac{\langle (s\bar{s})_P (s\bar{s})_S | V_a | \chi_{c1} \rangle}{\langle (q\bar{q})_P (q\bar{q})_S | V_a | \chi_{c1} \rangle}. \quad (6)$$

Following the above parametrization rule, we can write down the transition amplitudes for  $I = 0$  pseudoscalar ( $\eta$  or  $\eta'$ ) and scalar meson ( $f_0^i$ , with  $i = 1, 2, 3$  for  $f_0(1710)$ ,  $f_0(1500)$  and  $f_0(1370)$ , respectively) pair production as the following

$$\langle \eta f_0^i | V_a | \chi_{c1} \rangle = g(z_i \cos \alpha_P - y_i \sin \alpha_P R^2) \mathcal{F}(\mathbf{P}) \quad (7)$$

$$\langle \eta' f_0^i | V_a | \chi_{c1} \rangle = g(z_i \sin \alpha_P + y_i \cos \alpha_P R^2) \mathcal{F}(\mathbf{P}). \quad (8)$$

For  $\chi_{c1}$  decays into other channels with  $I \neq 0$ , e.g.  $\pi a_0$  and  $K\bar{K}_0^* + c.c.$ , the transition amplitudes are similar due to the exclusive contribution from Fig. 1(a):

$$\langle \pi^+ a_0^- | V_a | \chi_{c1} \rangle = \langle \pi^- a_0^+ | V_a | \chi_{c1} \rangle = \langle \pi^0 a_0^0 | V_a | \chi_{c1} \rangle = g \mathcal{F}(\mathbf{P}), \quad (9)$$

$$\langle K^+ K_0^{*-} | V | \chi_{c1} \rangle = \langle K^- K_0^{*+} | V | \chi_{c1} \rangle = \langle K^0 \bar{K}_0^{*0} | V | \chi_{c1} \rangle = \langle \bar{K}^0 K_0^{*0} | V | \chi_{c1} \rangle = g R \mathcal{F}(\mathbf{P}). \quad (10)$$

In the above equations,  $\mathcal{F}(\mathbf{P})$  is a commonly used form factor defined as follows,

$$\mathcal{F}^2(\mathbf{P}) \equiv |\mathbf{P}|^{2l} \exp(-\mathbf{P}^2/8\beta^2), \quad (11)$$

where  $\mathbf{P}$  and  $l$  are the three-vector momentum and the relative orbit angular momentum of the final-state mesons, respectively, in the  $\chi_{c1}$  rest frame. We adopt  $\beta = 0.5$  GeV, which is commonly adopted in the literature [5–8]. At leading order the decays of  $\chi_{c1} \rightarrow PS$  are via  $P$ -wave, i.e.  $l = 1$ . This form factor accounts for the size effects arising from the spatial wavefunction of the initial- and final-state mesons in the hadronizations.

### III. NUMERICAL RESULTS

So far, the only available experimental information was given by BES-II [27, 28], i.e.  $BR(\chi_{c1} \rightarrow K_J^{*0}(1430)\bar{K}^0 + c.c. \rightarrow K_s^0 K^+ \pi^- + c.c.) < 8 \times 10^{-4}$  and  $BR(\chi_{c1} \rightarrow K_J^{*+}(1430)K^- + c.c. \rightarrow K_s^0 K^+ \pi^- + c.c.) < 2.3 \times 10^{-3}$ , where the statistics were limited and the spin of  $K_J^{*0}(1430)$  has not been determined. In this process both  $K_0^*(1430)$  and  $K_2^*(1430)$  may have contributions. However, notice that the leading hadronic helicity-conserving amplitudes for  $\chi_{c1} \rightarrow K_0^{*0}(1430)\bar{K}^0 + c.c.$  and  $K_2^{*0}(1430)\bar{K}^0 + c.c.$  are from the  $S_z = 0$  components. It implies that the decay of  $\chi_{c1} \rightarrow K_2^{*0}(1430)\bar{K}^0 + c.c.$  via a  $P$  wave will be relatively suppressed by the Clebsch-Gordan coefficient,  $(20, 10|10)^2 = 2/5$  in comparison with that of  $K_0^{*0}(1430)\bar{K}^0 + c.c.$  This allows us to assume that the measured branching ratio is dominated by  $K_0^*(1430)\bar{K}^0 + c.c.$ , and set up upper limits of branching ratios for other decay channels. In another word, we can normalize the branching ratios of other decay channels to the  $K_0^{*0}(1430)\bar{K}^0 + c.c.$  channel (we take the lower limit as a conservative estimate), and inspect the variation of branching ratio fractions within a range of the SU(3) flavor symmetry breaking parameter  $R$ . Notice that the  $K_0^*(1430)$  decay is nearly saturated by the  $K\pi$  channel with  $BR(K_0^*(1430) \rightarrow K\pi) = (93 \pm 10)\%$ , which is larger than  $BR(K_2^*(1430) \rightarrow K\pi) = (49.9 \pm 1.2)\%$  [28]. We can simply take into account the charge conjugate by a factor of  $3/2$  for  $K_0^{*0}(1430)\bar{K}^0 + c.c. \rightarrow K_s^0 K^+ \pi^- + c.c.$  to obtain,  $BR(\chi_{c1} \rightarrow K_J^{*0}(1430)\bar{K}^0 + c.c.) < 1.2 \times 10^{-3}$  as the upper limit.

By studying this observable for different scalar meson mixing schemes, we can identify criteria for the determination of the quark contents of those scalar mesons. In turn, we expect to gain insights into their structures.

From Eqs. (7) and (10), we can take the branching ratio fraction

$$\gamma_\eta \equiv \frac{BR(\chi_{c1} \rightarrow \eta f_0^i)}{BR(\chi_{c1} \rightarrow K^0 \bar{K}_0^{*0} + c.c.)} = \frac{|\mathbf{P}_\eta| (z_i \cos \alpha_P - y_i \sin \alpha_P R^2)^2 \mathcal{F}^2(\mathbf{P}_\eta)}{2|\mathbf{P}_K| R^2 \mathcal{F}^2(\mathbf{P}_K)}, \quad (12)$$

where the factor 2 in the denominator is due to the charge conjugate factor for  $K^0 \bar{K}_0^{*0} + c.c.$  final states. Similarly, for the  $\eta'$  recoiling  $f_0^i$  we can define

$$\gamma_{\eta'} \equiv \frac{BR(\chi_{c1} \rightarrow \eta' f_0^i)}{BR(\chi_{c1} \rightarrow K^0 \bar{K}_0^{*0} + c.c.)} = \frac{|\mathbf{P}_{\eta'}| (z_i \sin \alpha_P + y_i \cos \alpha_P R^2)^2 \mathcal{F}^2(\mathbf{P}_{\eta'})}{2|\mathbf{P}_K| R^2 \mathcal{F}^2(\mathbf{P}_K)}, \quad (13)$$

and for the  $\pi^0 a_0^0$  channel we have

$$\gamma_\pi \equiv \frac{BR(\chi_{c1} \rightarrow \pi^0 a_0^0)}{BR(\chi_{c1} \rightarrow K^0 \bar{K}_0^{*0} + c.c.)} = \frac{|\mathbf{P}_\pi| \mathcal{F}^2(\mathbf{P}_\pi)}{2|\mathbf{P}_K| R^2 \mathcal{F}^2(\mathbf{P}_K)}. \quad (14)$$

For  $\chi_{c1} \rightarrow K^0 \bar{K}_0^{*0} + c.c.$ , the only parameter is  $R$  for which  $R \simeq f_\pi/f_K \sim 0.838$  is commonly adopted. Applying the experimental upper limit,  $BR(\chi_{c1} \rightarrow K_J^*(1430)^0 \bar{K}^0 + c.c.) < 1.2 \times 10^{-3}$  [27, 28], we can determine the basic transition strength  $g = 2.56 \times 10^{-2}$  via

$$\Gamma(\chi_{c1} \rightarrow K_J^*(1430)^0 \bar{K}^0 + c.c.) = \frac{|\mathbf{P}_K| g^2 R^2 \mathcal{F}^2(\mathbf{P}_K)}{12\pi M_{\chi_{c1}}^2}. \quad (15)$$

Also, the branching ratio of  $\chi_{c1} \rightarrow \pi^0 a_0^0$  can be estimated via Eq. (14), i.e.  $BR_{\chi_{c1} \rightarrow \pi^0 a_0^0} < 8.64 \times 10^{-4}$ .

Now we focus on Eqs. (12) and (13) to extract information about the scalar meson structures. The ratios  $\gamma_\eta$  and  $\gamma_{\eta'}$  are now explicit functions of the  $q\bar{q}$  mixing elements. We will analyze three typical mixing schemes in the literature. Predictions of the ratios would set up criteria for future experimental tests of those mixing scenarios.

Scheme-I:

A systematic study by Close *et al* based on a perturbation transition mechanism [5–8] determines the glueball- $q\bar{q}$  mixing matrix [8],

$$\hat{S}_1 = \begin{pmatrix} 0.36 & 0.93 & 0.09 \\ -0.84 & 0.35 & -0.41 \\ 0.40 & -0.07 & -0.91 \end{pmatrix}. \quad (16)$$

In this scheme the  $f_0(1710)$  is dominated by the  $s\bar{s}$  component, but its glueball component is also sizeable. In contrast, the  $f_0(1500)$  is dominated by  $G$  with a sizeable  $s\bar{s}$  component. The  $f_0(1370)$  is found dominated by the  $n\bar{n}$  ( $\equiv (u\bar{u} + d\bar{d})/\sqrt{2}$ ).

As mentioned earlier, the value  $R = 1$  corresponds to the SU(3) flavor symmetry limit, while  $R \simeq 0.838$  is the commonly adopted SU(3) flavor symmetry breaking scale. We thus consider a small variation of the parameter  $R$  in the range of  $R = 0.7 \sim 1.2$ , and plot the  $R$ -dependence of branching ratio fractions  $\gamma_\eta$  and  $\gamma_{\eta'}$  in Fig. 3 with the mixing matrix elements from Eq. (16) for the mixing Scheme-I. It is interesting to learn the following points about this scenario:

- Comparing the branching ratio fractions  $\gamma_\eta$  and  $\gamma_{\eta'}$ , we notice that the relative phases between the mixing matrix elements critically determine the production strengths of those scalars when recoil  $\eta$  or  $\eta'$ .
- Since the  $n\bar{n}$  dominates the  $f_0(1370)$  wavefunction and the  $s\bar{s}$  is negligibly small, the production rates of  $f_0(1370)$  are predicted to be larger than other channels in the vicinity of  $R \simeq 0.838$ .
- For the  $f_0(1710)$ , its production in association with  $\eta$  is relatively suppressed by the significant cancelation between the  $s\bar{s}$  and  $n\bar{n}$  components as shown by  $\gamma_\eta \simeq 0.03 \sim 0.15$ . In contrast, its production with  $\eta'$  is much more enhanced with  $\gamma_{\eta'} \simeq 0.13 \sim 0.31$ .
- The  $s\bar{s}$  and  $n\bar{n}$  components are compatible in the  $f_0(1500)$ , but out of phase. As a consequence, the production of the  $f_0(1500)$  seems to be unfavored in  $\chi_{c1} \rightarrow PS$  for the mixing Scheme-I. One also notices that both  $\gamma_\eta$  and  $\gamma_{\eta'}$  are insensitive to  $R$  as indicated by the dashed curves.

Scheme-II:

The second mixing scheme was provided by Cheng, Chua and Liu [10] based on the lattice QCD (LQCD) quenched calculations by Lee and Weingarten [9]. It was found that  $f_0(1710)$  is dominated by the glueball component, while  $f_0(1500)$  and  $f_0(1370)$  are dominated by  $s\bar{s}$  and  $n\bar{n}$ , respectively. This scenario is different from Ref. [18] where the glueball-dominant state is the  $f_0(1500)$ . The mixing scheme of Ref. [10] is similar to that of Ref. [9]. Therefore, we do not show the numerical survey of these two solutions, but only present the results for the typical solution from Ref. [9]

$$\hat{S}_2 = \begin{pmatrix} 0.859 & 0.302 & 0.413 \\ -0.128 & 0.908 & -0.399 \\ -0.495 & 0.290 & 0.819 \end{pmatrix}. \quad (17)$$

The predicted branching ratio fractions  $\gamma_\eta$  and  $\gamma_{\eta'}$  in terms of  $R$  are plotted in Fig. 4. In comparison with Fig. 3, the predicted decay pattern is quite different in the range of  $R > 0.8$ . In particular, one notices the strong suppression of

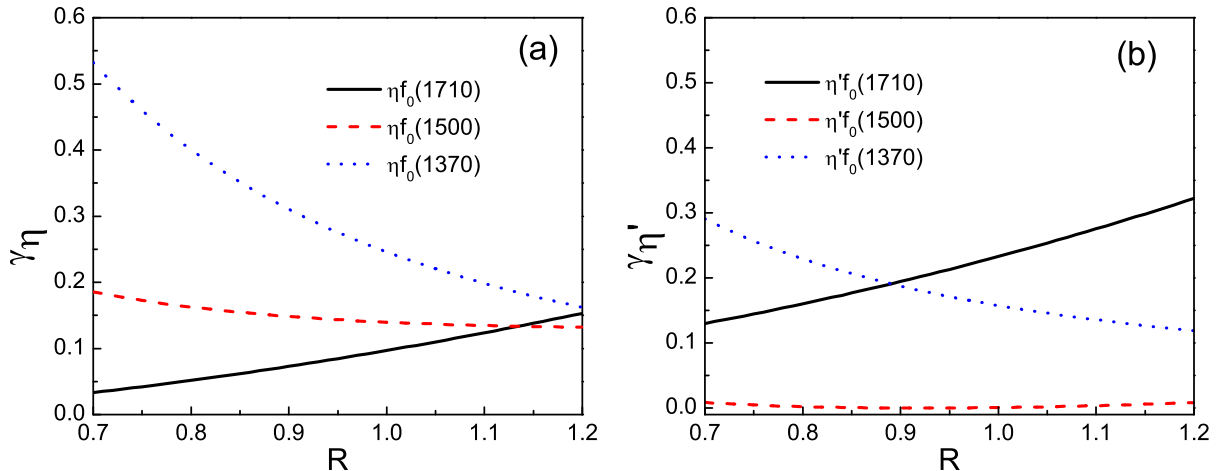


FIG. 3: The branching ratio fractions  $BR(\chi_{c1} \rightarrow \eta(\eta') f_0)/BR(\chi_{c1} \rightarrow K_J^*(1430)^0 \bar{K}^0 + c.c.)$  as a function of the parameter  $R$  is presented in this figure. In this case, the mixing matrix  $\hat{S}_1$  is used for scalar meson mixing. The solid line, dashed line and dotted line are the branching ratio fractions of  $\eta f_0(1710)$ ,  $\eta f_0(1500)$  and  $\eta f_0(1370)$  in Diagram (a). The cases in Diagram (b) are for  $\eta' f_0(1710)$ ,  $\eta' f_0(1500)$  and  $\eta' f_0(1370)$ .

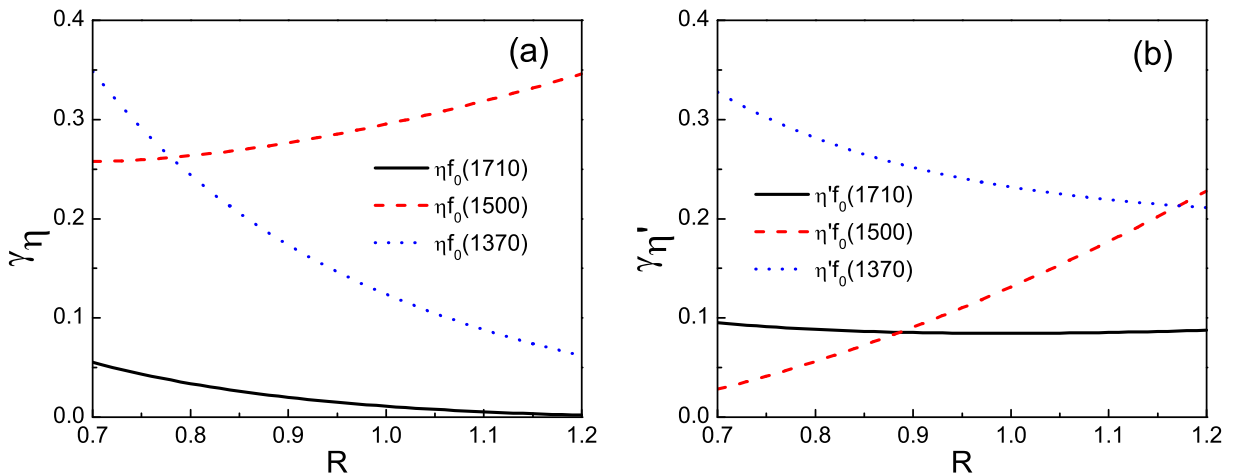


FIG. 4: The notations are similar to Fig.3 with the mixing matrix  $\hat{S}_2$ .

$\eta f_0(1710)$  in comparison with  $\eta f_0(1500)$  and  $\eta f_0(1370)$  in the vicinity of  $R \simeq 0.838$ . In the  $\eta'$  production channels, the  $\eta' f_0(1710)$  and  $\eta' f_0(1500)$  decays are relatively suppressed in comparison with  $\eta' f_0(1370)$ .

Interestingly, one notices that in case of  $R \simeq 0.7$ , the hierarchy of the branching ratio fractions between Figs. 3 and 4 are rather similar to each other. In such a situation, one may need additional observables to distinguish mixing schemes I and II.

Scheme-III:

Giacosa *et al.* obtained four possible solutions by fitting the masses and decay widths of those three  $f_0$  states in an effective chiral approach [26]. Their two typical solutions, i.e.  $\hat{S}_{3a}$  and  $\hat{S}_{3b}$  were obtained without direct glueball

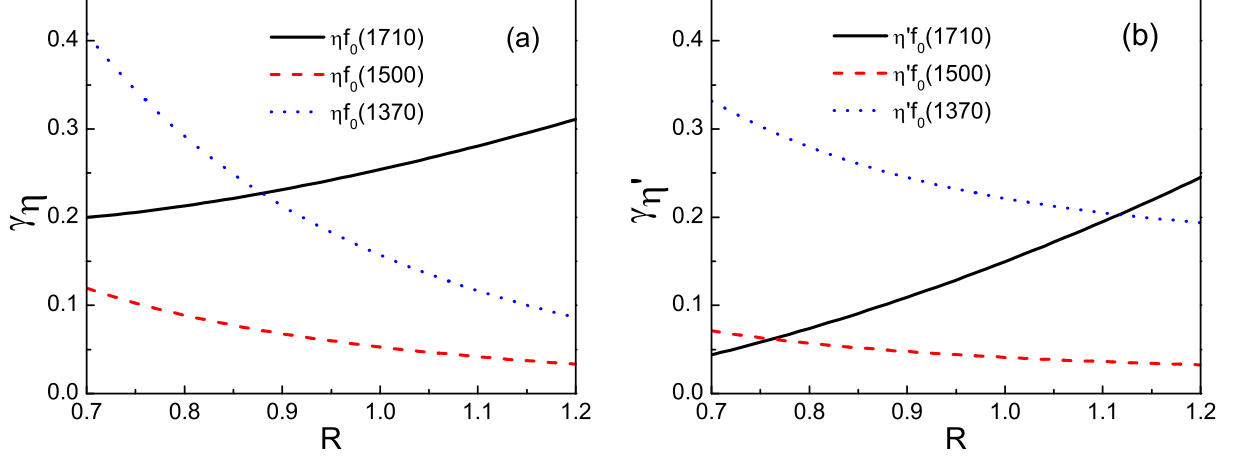


FIG. 5: The notations are similar to Fig.3 with the mixing matrix  $\hat{S}_{3a}$ .

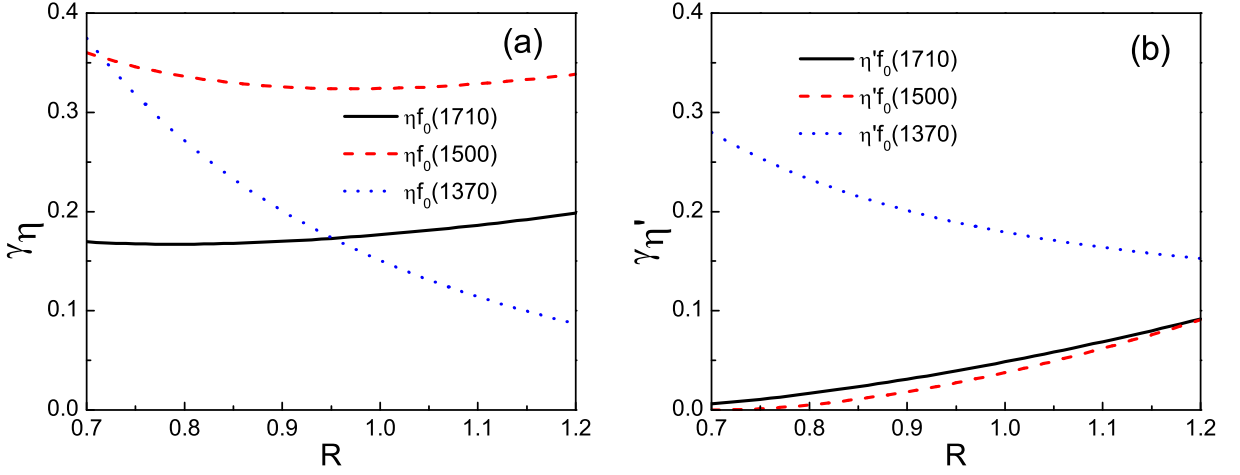


FIG. 6: The notations are similar to Fig.3 with the mixing matrix  $\hat{S}_{3b}$ .

decays, and have the following expressions,

$$\hat{S}_{3a} = \begin{pmatrix} -0.06 & 0.97 & -0.24 \\ 0.89 & -0.06 & -0.45 \\ 0.45 & 0.24 & 0.86 \end{pmatrix}, \quad (18)$$

and

$$\hat{S}_{3b} = \begin{pmatrix} -0.68 & 0.67 & -0.30 \\ 0.49 & 0.72 & -0.49 \\ 0.54 & 0.19 & 0.81 \end{pmatrix}. \quad (19)$$

These two solutions were extracted with the OZI-rule violation parameters  $r = 1.93 \pm 0.29$  and  $-2.07 \pm 0.79$  determined in  $J/\psi \rightarrow \phi f_0^i$  and  $\omega f_0^i$ , and they are both of order of one. Such a large OZI-rule violation parameter in  $J/\psi \rightarrow \phi f_0^i$

TABLE I: The upper limits of the branching ratios  $\chi_{c1} \rightarrow \eta f_0$  is presented with the SU(3) breaking parameter  $R \equiv f_\pi/f_K \simeq 0.838$ . The experimental value  $BR(\chi_{c1} \rightarrow K_J^*(1430)^0 \bar{K}^0 + c.c.) < 1.2 \times 10^{-3}$  [28] is used to predict the upper limits.

| $BR(\chi_{c1} \rightarrow PS)$ | $\hat{S}_1$           | $\hat{S}_2$           | $\hat{S}_{3a}$        | $\hat{S}_{3b}$        |
|--------------------------------|-----------------------|-----------------------|-----------------------|-----------------------|
| $\eta f_0(1710)$               | $7.2 \times 10^{-5}$  | $3.3 \times 10^{-5}$  | $2.63 \times 10^{-4}$ | $2.03 \times 10^{-4}$ |
| $\eta f_0(1500)$               | $1.88 \times 10^{-4}$ | $3.23 \times 10^{-4}$ | $9.69 \times 10^{-5}$ | $3.98 \times 10^{-4}$ |
| $\eta f_0(1370)$               | $4.32 \times 10^{-4}$ | $2.55 \times 10^{-4}$ | $3.08 \times 10^{-4}$ | $2.90 \times 10^{-4}$ |
| $\eta' f_0(1710)$              | $2.10 \times 10^{-4}$ | $1.04 \times 10^{-4}$ | $1.04 \times 10^{-4}$ | $2.70 \times 10^{-5}$ |
| $\eta' f_0(1500)$              | $4.89 \times 10^{-7}$ | $8.27 \times 10^{-5}$ | $6.38 \times 10^{-5}$ | $1.09 \times 10^{-5}$ |
| $\eta' f_0(1370)$              | $2.51 \times 10^{-4}$ | $3.21 \times 10^{-4}$ | $3.17 \times 10^{-4}$ | $2.61 \times 10^{-4}$ |

and  $\omega f_0^i$  confirms the result of Ref. [8]. In  $\chi_{c1}$  decays, as discussed in the Introduction, the OZI rule and Landau-Yang suppression together would lead to a small value for the OZI-rule violation parameter. It means that we have neglected contributions from Fig. 1(d).

The main difference between these two solutions,  $\hat{S}_{3a}$  and  $\hat{S}_{3b}$ , lies in the different prescriptions of the glueball and  $s\bar{s}$  contents for the  $f_0(1710)$  and  $f_0(1500)$ , respectively. Compared with mixing scheme-I and II, it shows that  $\hat{S}_{3a}$  is similar to  $\hat{S}_1$  of Ref. [8], but the second solution  $\hat{S}_{3b}$  is quite different.

In Figs. 5 and 6, the predicted branching ratio fractions are presented for those two solutions  $\hat{S}_{3a}$  and  $\hat{S}_{3b}$ , respectively. Their different prescriptions lead to drastic changes of the production rate for the  $f_0(1500)$  around  $R = 0.838$ . In the mixing scheme of  $\hat{S}_{3a}$ , the decay channel  $\eta f_0(1500)$  is suppressed in comparison with  $\eta f_0(1710)$  and  $\eta f_0(1370)$ , while in  $\hat{S}_{3b}$  it is strongly enhanced to be larger than the other two channels. The  $R$  dependence of  $\gamma_\eta$  and  $\gamma_{\eta'}$  can also be observed in these two mixing schemes.

Interestingly, in the vicinity of  $R \simeq 0.838$  the decay patterns illustrated by those mixing schemes (four different mixing matrices) can still be distinguished. As mentioned earlier that the structure of mixing matrices,  $\hat{S}_{3a}$  and  $\hat{S}_1$ , are similar to each other, we can see that their predictions for the production of  $f_0(1710)$  are quite different. For instance, it shows that the production of  $f_0(1710)$  in association with  $\eta$  is more favored than with  $\eta'$  in  $\hat{S}_{3a}$ , and it is opposite in  $\hat{S}_1$ .

In Table I, we list the branching ratios of  $\chi_{c1} \rightarrow \eta(\eta')f_0$  with  $R = 0.838$  as a predictions from those mixing schemes. Combining what illustrated in Figs. 3-6, we learn the following points concerning the production of the scalars:

- The  $f_0(1370)$  is dominated by the  $n\bar{n}$  component in all those schemes. Nevertheless, all those mixing schemes find that the relatively small  $s\bar{s}$  component is in phase to the dominant  $n\bar{n}$ . As a consequence, the predicted branching ratios of both  $\eta f_0(1370)$  and  $\eta' f_0(1370)$  turn out to have a stable behavior.
- For the  $f_0(1500)$ , sensitivities of the branching ratio fractions  $\gamma_\eta$  and  $\gamma_{\eta'}$  to its quark contents can be seen. The predicted branching ratios of  $\chi_{c1} \rightarrow \eta f_0(1500)$  are at the order of  $10^{-4}$  which could be accessible at BES-III. One also notices that the  $\eta' f_0(1500)$  channel is relatively suppressed in all those mixing schemes since the  $n\bar{n}$  and  $s\bar{s}$  have opposite signs in the mixing schemes  $\hat{S}_1$ ,  $\hat{S}_2$  and  $\hat{S}_{3b}$ , while in  $\hat{S}_{3a}$  the  $n\bar{n}$  and  $s\bar{s}$  both are small.
- The branching ratios of the  $\eta f_0(1710)$  and  $\eta' f_0(1710)$  are also sensitive to the mixing schemes. Combine together the decay patterns of other scalars, it is possible to distinguish those mixing schemes in experiment.

It should also be pointed that experimental analysis may become much more complicated due to the background contributions to the final states. For the  $PS$  channel, the final-state particles involve  $\eta\pi\pi$ ,  $\eta K\bar{K}$ ,  $\eta'\pi\pi$ , and  $\eta'K\bar{K}$  etc. As shown by the recent measurement from CLEO-c [29] that the  $\eta\pi\pi$  and  $\eta'\pi\pi$  channels may not be suitable for the search for the scalar meson signals due to large background contributions. In contrast, the  $\eta K\bar{K}$  and  $\eta'K\bar{K}$  channels may be more sensitive to the scalar meson productions. With the high statistics measurement at BEPC-II/BES-III, we anticipate that progress can be made in the study of the scalar meson spectrum.

One should also be cautioned that the dominance of the hair-pin diagram is a crucial assumption in this study. A better respect of this assumption may be achieved in the bottomonium sector, namely, in  $\chi_{b1} \rightarrow PS$ . Unfortunately, there are no experimental data available at this moment for this channel. The future LHCb experiment may be able to provide additional information about the nature of those scalar mesons.



#### IV. SUMMARY

To summarize, we show that the decay of  $\chi_{c1} \rightarrow PS$  could be an ideal channel for probing the quark contents of the those scalar mesons in the mass region of  $1\sim 2$  GeV, i.e.  $f_0(1370)$ ,  $f_0(1500)$  and  $f_0(1710)$ . Because of the suppression from the Landau-Yang theorem to those gluon loop diagrams, this decay channel at leading order should be dominated by the pQCD hair-pin transition process. It thus allows us to tag the quark contents of the final state scalars by the quark components of the recoiled  $\eta$  and  $\eta'$ . A prediction for the upper limits of the branching ratios of  $\chi_{c1} \rightarrow \eta f_0^i$  and  $\eta' f_0^i$  can be made with the available experimental data and based on different scalar mixing schemes in the literature. It can be expected that a precise measurement of  $\chi_{c1} \rightarrow PS$  will be able to distinguish those model prescriptions for the glueball- $q\bar{q}$  mixing scenario and provide further evidence for the scalar glueball candidates.

#### V. ACKNOWLEDGEMENT

Q.Z. is indebted to K.-T. Chao, F.E. Close, M. Shepherd, J.-X. Wang, and B.-S. Zou for useful discussions. Authors thank X.-Y. Shen, and Z.-T. Sun for useful comments on an early draft. This work is supported, in part, by National Natural Science Foundation of China (Grant Nos. 11035006 and 10947007), Chinese Academy of Sciences (KJ CX2-EW-N01), Ministry of Science and Technology of China (2009CB825200), and the Natural Science Foundation of Shandong Province (Grant No. ZR2010AM011).

- 
- [1] N. Brambilla *et al.* [Quarkonium Working Group Collaboration], hep-ph/0412158.
  - [2] N. Brambilla, S. Eidelman, B. K. Heltsley, R. Vogt, G. T. Bodwin, E. Eichten, A. D. Frawley and A. B. Meyer *et al.*, Eur. Phys. J. C **71**, 1534 (2011) [arXiv:1010.5827 [hep-ph]].
  - [3] M. Ablikim *et al.* [BES Collaboration], Phys. Lett. B **607**, 243 (2005) [hep-ex/0411001].
  - [4] M. Ablikim *et al.* [BES Collaboration], Phys. Lett. B **603**, 138 (2004) [hep-ex/0409007].
  - [5] C. Amsler and F. E. Close, Phys. Lett. B **353**, 385 (1995) [arXiv:hep-ph/9505219].
  - [6] C. Amsler and F. E. Close, Phys. Rev. D **53**, 295 (1996) [arXiv:hep-ph/9507326].
  - [7] F. E. Close and A. Kirk, Phys. Lett. B **483**, 345 (2000) [arXiv:hep-ph/0004241].
  - [8] F. E. Close and Q. Zhao, Phys. Rev. D **71**, 094022 (2005) [arXiv:hep-ph/0504043].
  - [9] W. J. Lee and D. Weingarten, Phys. Rev. D **61**, 014015 (2000) [arXiv:hep-lat/9910008].
  - [10] H. Y. Cheng, C. K. Chua and K. F. Liu, Phys. Rev. D **74**, 094005 (2006) [arXiv:hep-ph/0607206].
  - [11] G. S. Adams *et al.* [CLEO Collaboration], Phys. Rev. D **75**, 071101 (2007) [arXiv:hep-ex/0611013].
  - [12] J.Z. Bai *et al.* [BES Collaboration], Phys. Rev. D **60**, 072001 (1999).
  - [13] M. Ablikim *et al.* [BES Collaboration], Phys. Rev. D **70**, 092003 (2004).
  - [14] M. Ablikim *et al.* [BES Collaboration], Phys. Lett. B **630**, 7 (2005) [arXiv:hep-ex/0506045].
  - [15] J.Z. Bai *et al.* [BES Collaboration], Phys. Rev. Lett. **81**, 3091 (1998).
  - [16] J.Z. Bai *et al.* [BES Collaboration], Phys. Rev. D **67**, 032004 (2003).
  - [17] M. Ablikim *et al.* [BES Collaboration], Phys. Rev. D **72**, 092002 (2005) [arXiv:hep-ex/0508050].
  - [18] Q. Zhao, Phys. Lett. B **659**, 221 (2008) [arXiv:0705.0101 [hep-ph]].
  - [19] Q. Zhao, Phys. Rev. D **72**, 074001 (2005) [hep-ph/0508086].
  - [20] C. -N. Yang, Phys. Rev. **77**, 242 (1950).
  - [21] H. W. Huang and K. T. Chao, Phys. Rev. D **54**, 6850 (1996) [Erratum-ibid. D **56**, 1821 (1997)] [arXiv:hep-ph/9606220].
  - [22] H. Q. Zhou, R. G. Ping and B. S. Zou, Phys. Lett. B **611**, 123 (2005) [arXiv:hep-ph/0412221].
  - [23] G. Li, Q. Zhao and C. H. Chang, J. Phys. G **35**, 055002 (2008) [arXiv:hep-ph/0701020].
  - [24] F. E. Close and N. A. Tornqvist, J. Phys. G **28**, R249 (2002) [arXiv:hep-ph/0204205].
  - [25] E. Klempt and A. Zaitsev, Phys. Rept. **454**, 1 (2007) [arXiv:0708.4016 [hep-ph]].
  - [26] F. Giacosa, T. Gutsche, V. E. Lyubovitskij and A. Faessler, Phys. Rev. D **72**, 094006 (2005) [arXiv:hep-ph/0509247].
  - [27] M. Ablikim *et al.* [BES Collaboration], Phys. Rev. D **74**, 072001 (2006) [hep-ex/0607023].
  - [28] K. Nakamura *et al.* [Particle Data Group], J. Phys. G **37**, 075021 (2010).
  - [29] G. S. Adams *et al.* [CLEO Collaboration], Phys. Rev. D **84**, 112009 (2011) [arXiv:1109.5843 [hep-ex]].